

# Measurements on the Mobility of Ions and Ionic Clusters in Gases with the 20 msec Isomer of $^{24m}\text{Na}^+$ as Tracer

**B. Abmayr, E. Huenges, H. Morinaga**

Physics Department, Technische Universität München, 8046 Garching, Germany

**A. Kasuya, Y. Nishina**

Institute for Materials Research, Tohoku University, Sendai 980, Japan

**Mr. Kotajima + Students**

Department of Nuclear Engineering, Tohoku University, Sendai 980, Japan

**Mr. Ohtsuki + Mr. Matsumoto**

Laboratory of Nuclear Science, Tohoku University, Sendai 980, Japan

**Abstract.** Mobilities of sodium ions and their clusters in different gases have been measured by gamma-ray spectrometry using the 20 ms isomeric state of  $^{24}\text{Na}$  as tracer. This isomer is obtained through the  $\beta^-$ -decay of  $^{24}\text{Ne}$ , which was produced by bombarding  $^{22}\text{Ne}$  with the 7 MeV triton beam of a cyclotron. In a later experiment  $^{24}\text{Ne}$  was produced by irradiation of a target containing  $^{26}\text{Mg}$  with the bremsstrahlung of a 60 MeV electron beam of a linear accelerator.

This new technique of measurement can be used to determine the mobility of sodium ions in non-reacting gases of a pressure higher than 1 mbar. Measurements have been carried out in gases of pressures ranging from 6 mbar to 1000 mbar under an electric field up to 250 V/cm at room temperature. The measured mobility of  $^{24}\text{Na}^+$  in pure neon gas at 1000 mbar was determined to be  $3.2 \text{ cm}^2/\text{Vs}$ . This value is much lower than the zero field mobility of about  $8.5 \text{ cm}^2/\text{Vs}$  measured by Tyndall [1] and Akridge [2].

A small amount of polar molecules such as water or ethanol introduced into the drift tube causes their clustering with the sodium ions through monopole-dipole interaction, resulting in a strong decrease in the mobility. This clustering effect has been studied for various combinations of polar

molecules and inert gases.

The usable pressure range from 1 mbar to high pressures in the range of some hundred bars is interesting because most other methods for cluster studies do not work at such high pressures. With this method it should be possible to measure the mobility change of sodium ions towards the condensation point and eventually even towards the critical point.

**PACS: 34.90.+q**

## 1. Introduction

$^{24}\text{Ne}$  is  $\beta^-$  instable with a half-life-time of 3 minutes by emitting two gamma rays with energies of 874 keV and 472 keV. The former decay is prompt, but the latter is delayed with a half-life-time of 20 msec (fig. 1).

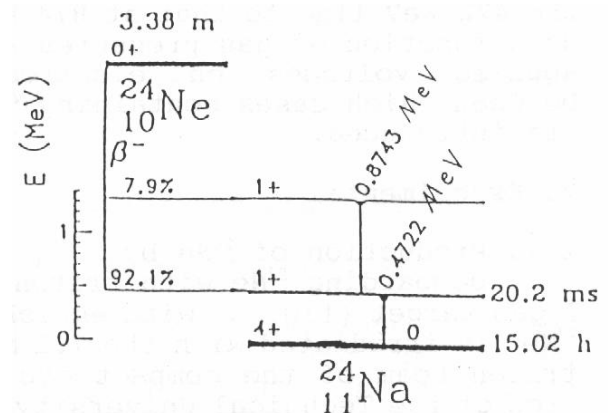


Fig. 1: Decay scheme of  $^{24}\text{Ne}$  [3].

This fact gives us an excellent opportunity to use  $^{24}\text{Ne}$  as a generator of this 472 keV isomeric state of  $^{24}\text{Na}$  which can be used as a tracer to measure phenomena which occur in the time scale of about 20 milliseconds.

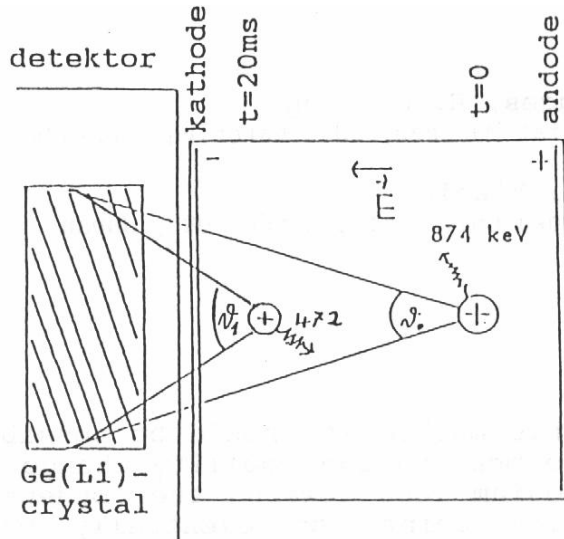


Fig. 2: Change in the probability of detecting ions moving in an electrical field.  $t=0$ : 874 keV photon.  $t=20\text{ms}$ : 472 keV with larger detection probability

We have measured drift velocities of  $\text{Na}^+$  ions and of clusters built on these ions by measuring the change in the solid angle subtended by a Ge(Li) gamma ray detector when the sodium ions (clusters) are accelerated by electric fields (Fig. 2). We have measured the ratio of intensity of the 472 keV line to that at 874 keV as a function of gas pressures and applied voltages on electrodes between which gases containing  $^{24}\text{Ne}$  are introduced.

## 2. Experimental

Two different methods for production of  $^{24}\text{Ne}$  have been used.

### 2.1. Production of $^{24}\text{Ne}$ by bombarding $^{22}\text{Ne}$ with tritons

A gas target (fig. 3) with enriched  $^{22}\text{Ne}$  is irradiated with the 7.2 MeV triton beam of the compact cyclotron of the Technical University of Munich [2]. When enough  $^{24}\text{Ne}$  is produced, the gas is

pumped into the ion acceleration chamber in another room in order to avoid the neutrons and the background activity caused by the cyclotron. The measurement of the gamma spectrum is started after applying the electrical field in the ion acceleration chamber. After the measurement the gas is pumped back to the irradiation chamber and a new cycle of experiment begins.

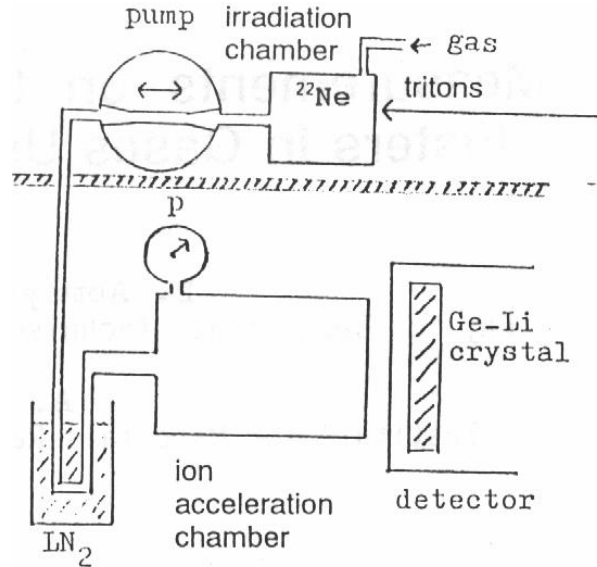


Fig. 3: Schematic picture of the experimental setup

### 2.2. Production of $^{24}\text{Ne}$ by irradiation of $^{26}\text{Mg}$ with gamma rays

At the electron linear accelerator of the Tohoku University Sendai the 60 MeV electrons are stopped by a platinum stopper. The bremsstrahlung is used to irradiate a magnesium oxide powder. Instead of pure magnesium we use  $\text{MgO}$  for safety reasons. Besides several other reactions  $^{24}\text{Ne}$  is produced from  $^{26}\text{Mg}$  by absorption of a gamma quantum and emission of two protons. We use very fine  $\text{MgO}$  powder, because the produced  $^{24}\text{Ne}$  has a range of about  $1\ \mu\text{m}$  in the material. In order to get a high yield most of the  $^{24}\text{Ne}$  should come out of the  $\text{MgO}$  grains. After filling up its electron shell  $^{24}\text{Ne}$  is a neutral atom and is transported by a carrier gas to the ion acceleration chamber.

### 2.3. Comparison of both methods for production of $^{24}\text{Ne}$

In both cases besides  $^{24}\text{Ne}$  only few other radioactive isotopes arrive at the ion acceleration chamber together with the pumped gas. Therefore the measurements of the gamma spectra are not hindered much by other activities.

Using a  $^{22}\text{Ne}$  gas target the producible  $^{24}\text{Ne}$  activity per volume is rather limited, depending on the available intensity of the triton beam, because the produced  $^{24}\text{Ne}$  cannot be separated from the original  $^{22}\text{Ne}$ . Using a magnesium target a gas highly enriched with  $^{24}\text{Ne}$  is produced in the irradiation chamber because the original material is solid. But for transportation to the ion acceleration chamber a carrier gas is necessary, which dilutes this high concentration of  $^{24}\text{Ne}$ . If one uses a good combination for the carrier gas, it will be possible to increase the concentration of  $^{24}\text{Ne}$  in the ion acceleration chamber, if a part of the carrier gas is removed by a gas trap. Until now in both ways of production the yield of  $^{24}\text{Ne}$  was always large enough for the measurements we wanted to do. But for later applications of this method it could be necessary to work with higher concentrations of  $^{24}\text{Ne}$ .

Another advantage of the production at an electron accelerator is that it is easier to find electron accelerators than triton accelerators.

### 2.4. Measurements

When enough  $^{24}\text{Ne}$  is produced in the irradiation chamber, the  $^{24}\text{Ne}$  is pumped together with the carrier gas into the ion accelerating chamber. The measurement of the gamma spectrum starts just after applying the electrical field in the ion accelerating chamber. From the measured gamma ray spectra, the ratio of the peak area of both gamma lines at 472 keV and 874 keV are calculated. The peak area ratio  $R$  contains the

information essential for calculating the ion mobility. The parameters are the pressure  $p$  in the ion accelerating chamber and the electrical field  $E$  between the electrodes. The ion acceleration chamber is designed such that the change of the peak area ratio  $R$  by movement of the ions becomes large. The chamber is a cylinder with radius 3 cm and height 6 cm. The voltage is applied between the top and the bottom plate. The wall between top and bottom is kept at the medium potential. Of course, the chamber is positioned as close to the gamma detector as possible.

### 2.5. Analysis of Experimental Data

The ion mobility is determined by fitting the experimental curve of the peak area ratio  $R$  versus  $E/p$  to a numerically calculated one. This theoretical curve is calculated in the following way.

The detection probability for gamma quanta at different positions in front of the gamma detector is measured by using a calibration source. Because of the relatively high pressure the ion movement by diffusion may be neglected, and the ions move along the electrical field lines with a drift velocity  $v$ , which is directly proportional to  $E/p$  [5]. This leads to  $v = \mu_0 * E/p$ , where  $\mu_0$  is the mobility at  $p = 1013$  mbar. The electrical field (fig. 4)

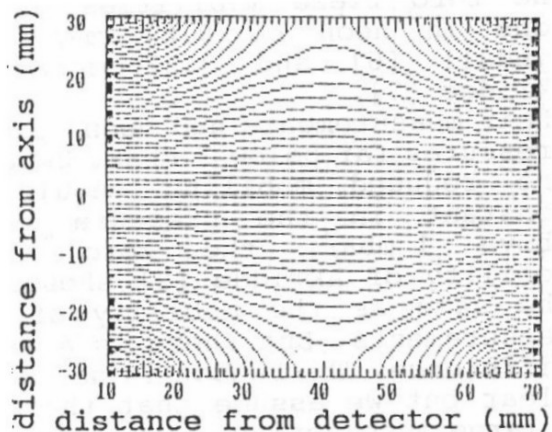


Fig. 4: Electric field lines in the cylindrical ion acceleration chamber.

in the ion acceleration chamber is calculated by a numerical solution of Poisson's equation.

Recombination of the ions in the gas is excluded due to the small ionization density in the chamber. Therefore each ion which comes into being at any place of the chamber will move on a path  $s(t)$  along one field line to the wall of the chamber and stay there at least until the isomeric state decays.

The detection probability for an ion that arrives at the place  $(x_0, y_0, z_0)$  at  $t=0$  is given through the following equation:

$$P_{\mu}(x_0, y_0, z_0) = \frac{\int_0^{\infty} A(t) P_{\mu}(s(t)) dt}{\int_0^{\infty} A(t) dt} \quad (1)$$

$A(t)$  is the exponential decay activity of the isomeric state and  $P_{\mu}$  is the detection probability for a fixed mobility  $\mu$  depending on the path  $s(t)$ .

In order to get the normalized peak area ratio one must integrate over the whole chamber and normalize by the value without ion movement. By this calculation for each mobility a curve like the one shown in fig. 5 is obtained. Now this numerically calculated curve is fitted to the experimental curve by varying the mobility  $\mu$ . Fig. 5 shows the result of fitting.

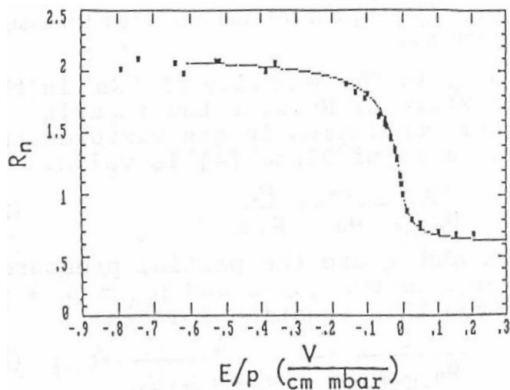


Fig. 5: Comparison of the experimental curve with the best fitting numerically calculated curve

### 3. Results and Discussions

#### 3.1. Measurements with Neon

##### 3.1.1. Unpurified Neon Gas

The first measurements have been performed with neon gas without purifying the gas, gas system and ion acceleration chamber. The result is shown in fig. 5. Out of this curve  $\mu_0 = 1.65 \text{ cm}^2/\text{Vs}$  is obtained. It is difficult to determine the error of all these measurements because the analysis of the data is rather complicated. However, for the mobility values we estimate the maximum error to be less than 10%.

In order to get information about the effects of the impurities on the mobility more measurements have been done at lower pressures of 6, 12, 20, 32 and 46 mbar (see fig 6).

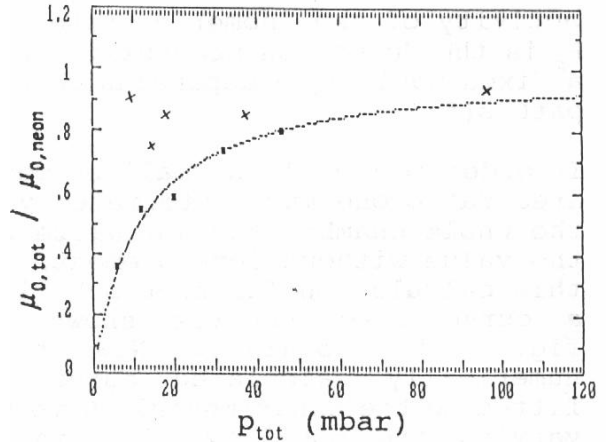


Fig. 6: Reduced ion mobilities at different pressures in unpurified (squares with fitting curve) and purified (crosses) neon gas

$\mu_{0,tot}$  is the mobility of  $^{24}\text{Na}^+$  in the mixture of Ne with the impurities. For mobilities in gas mixtures the formula of Blanc [6] is valid:

$$\frac{P_{tot}}{\mu_{0,tot}} = \frac{P_1}{\mu_{0,1}} + \frac{P_2}{\mu_{0,2}} \quad (2)$$

$p_1$  and  $p_2$  are the partial pressures of the two gases and  $p_{tot} = p_1 + p_2$ . From this equation follows:

$$\frac{1}{\mu_{0,tot}} = \frac{1}{\mu_{0,neon}} + \frac{1}{(\mu_{0,neon} - 1) * p_i} * P_{tot} \quad (3)$$

Index  $i$  stands for impurity.

Fig. 6 contains the best fitting curve which is obtained, if  $(\mu_{0,neon} / \mu_{0,i} - 1) * p_i = 12$  mbar. If, for example,  $p_i = 1$  mbar, the ion mobility in the impurity gas would be  $1/13 \mu_{0,neon}$ . More information cannot be obtained with certainty. But it is reasonable to assume that most of the impurities will be nitrogen, oxygen and water vapour. In all these gases the mobility should be much larger than only a thirteenth of the one in neon. Therefore the water molecules are expected to build clusters together with the ions because of their large permanent dipole moment. These ion clusters have much lower mobilities than free ions, what Munson [7] and Tyndall already had seen.

#### 4.1.2. Purified Neon Gas

After improving the experimental setup the measurement chamber can be baked out at 200°C and the incoming gas can be cleaned by passing a liquid nitrogen cooled trap.

Again we measured with neon gas at different pressures. The result is shown in fig. 6. The effect of gas cleaning is clear. The ion mobility decreases only slowly with decreasing pressure and the mobility value at 1000 mbar increased to  $\mu_0 = 3.2 \text{ cm}^2/\text{Vs}$ , which is nearly double the value of the mobility in unpurified neon gas. This value should be compared with the zero field mobilities of  $\text{Na}^+$  ions in neon of  $8.87 \text{ cm}^2/\text{Vs}$  by Tyndall [1] and  $8.27 \text{ cm}^2/\text{Vs}$  by Akridge [2].

They measured at pressures far below 1 mbar. Because the reduced mobility should be constant in the pressure range above 1 mbar, the zero field mobility of Akridge should be the same as the mobility of our measurements. But there is a large difference. The reason is not quiet clear but we assume that there is a large interaction between the ion and environmental gas atoms due to monopole-induced-

dipole forces. This interaction increases fast with decreasing distances between ions and atoms and therefore also with increasing pressure. This would also explain the slight decrease in the mobility with decreasing pressures in fig. 6. Due to this interaction there may be even in the rare gas neon temporary clustering of neutral neon atoms on the ions at room temperature at such high pressures we used.

But we cannot exclude that in spite of purification there remain some impurities in the gas, because we can not analyze the gas in the ion acceleration chamber. Probably most water molecules are removed by the liquid nitrogen trap, but oxygen and nitrogen molecules may pass the trap.

#### 4.2. Measurements with He - Ne Mixtures

Because the gas is purified with a liquid nitrogen trap there are only few gases which can be used for measurements with purified gas, i.e. helium, neon and hydrogen. Some measurements have been done with mixtures of helium and neon. At both mixture ratios (50% He with 50% Ne and 93% He with 7% Ne) we got using Blanc's mixture formula:

$$\mu_{0,heilmium} / \mu_{0,neon} = 2.4$$

This is close to Akridges [2] ratio of 2.74 for the zero field mobilities in the two gases, if we consider the errors and small rest impurities which decrease this ratio as Munson [7] has shown.

#### 4.3. Measurements with Ne-Ethanol Mixtures

In order to test possible applications of the tracer method a series of mobility measurements has been performed in different mixtures of neon and ethanol. The different ethanol partial pressures are obtained by cooling or heating the whole ion acceleration chamber. The ethanol partial pressure is the vapour

pressure above the liquid ethanol at the used temperature. Into this system we pump the necessary amount of not irradiated neon gas and afterwards the irradiated neon gas. Fig. 7 shows the results of the measurements.

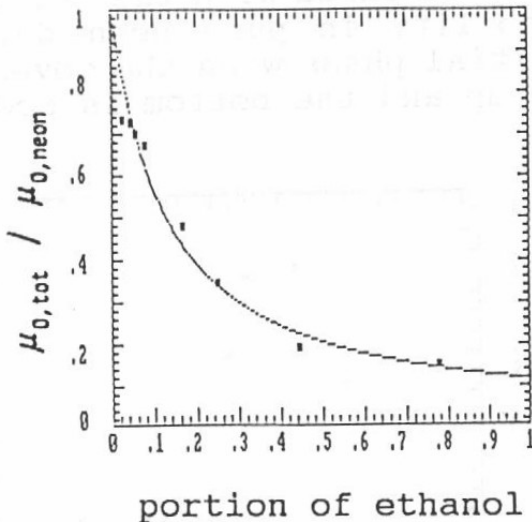


Fig. 7: Relative mobilities of Na+ ions in different neon-ethanol mixtures with best fitting curve for  $\mu_{0,neon} / \mu_{0,ethanol} = 9$ .

$\mu_{0,tot} / \mu_{0,neon}$  is shown depending on the ethanol concentration. Using Blanc's formula the best fitting curve is calculated for

$$\mu_{0,neon} / \mu_{0,ethanol} = 9.$$

One of the reasons for this low mobility value in ethanol vapour is the large cross section of the ethanol molecule, which exists of nine atoms. But this is not enough to explain such a strong decrease of the mobility. Cluster growth by attachment of ethanol molecules to the ions will decrease the ion mobility efficiently. Also the easy excitability of ethanol molecules may contribute to the lowering of the mobility.

#### 4.4. Mobility Measurements in a Diffusion Cloud Chamber

In order to see what happens to the ion mobility in a region of supersaturation an experiment with a diffusion cloud chamber has been performed [8], [9]. An electric field is applied in the lower third of our diffusion cloud

chamber where the supersaturation should take place. The irradiated neon gas is put into the cloud chamber during its performance. Neon serves as carrier gas. We use pure ethanol as liquid and diffusion gas. The input neon gas pressure is measured. The mean ethanol partial pressure is calculated from the measured total pressure. The gas partial pressures depend strongly on the height in the chamber due to the temperature gradient. In order to generate the electric field for the ion movement different things have to be fixed inside the chamber. Due to condensation on this material it is not possible to run our diffusion cloud chamber in a steady state with a constant supersaturated region. But we can show the behaviour of the ion mobility compared with the value of the mobility in pure neon during the initial phase when the cover is heated up and the bottom is cooled down.

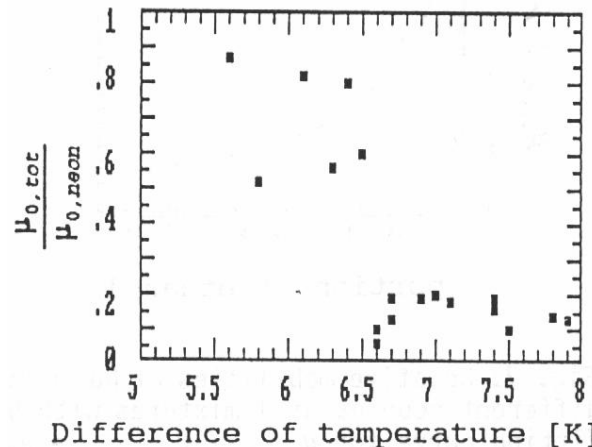


Fig. 8: Relative ion mobilities in a diffusion cloud chamber depending on the temperature gradient in the chamber.

Fig. 8 shows the mobility depending on the gradient of the temperature. The temperatures are measured a little below the cover plate containing the liquid ethanol and a little above the bottom. The difference of these temperatures is plotted on the x-axis. The errors of the mobility measurements in the cloud chamber are rather large due to a disadvantageous geometry for the

gamma measurements caused by the construction of any cloud chamber. Therefore the values of the mobility scatter rather much. But the figure shows that at a certain temperature gradient in the cloud chamber the ion mobility decreases suddenly. This effect can only be explained if the supersaturation suddenly exceeds a value above which the sodium ions cause rapid condensation of the ethanol vapour. The ions grow quickly (compared to the trace time of 20 msec) to large clusters or even small droplets, which causes a large decrease in the mobility.

The result of the cloud chamber experiments is clear: This method for mobility measurements can be used to detect clustering effects in such a condition critically close to condensation.

## 5. Concluding Remarks

The introduced tracer method is well suited for measurements on the mobilities of positive charged sodium ions in gases with pressures larger than 1 mbar. Measurements at lower pressures should be possible after improving the experimental setup. But the increasing movement by diffusion would destroy the indirect proportionality of the mobility to the pressure. Also the collision rate goes down and the ions will no longer move along the electrical field lines. The movement caused by the recoil of the  $\beta$  decay will increase too. All these facts together will effort another method for calculating the movement of the ions which is necessary for the analysis of the experimental data.

The usable pressure range is interesting because most other methods for cluster studies don't work at such high pressures. Measurements up to high pressures of some 100 bars are possible with this method. With a proper setup studies on the mobility change towards the condensation point and eventually towards the critical

point are possible with this method.

## Acknowledgement

This work was supported by the Japan Society for Promotion of Science.

## References

1. Tyndall A.M., Powell C.F.: Proceedings of the Royal Society of London **A 136**, 145 (1932)
2. Akridge G.R. et.al.: J. Chem. Phys. **62**, 4578 (1975)
3. Lederer C.M., Shirley V.S.: "Table of Isotops", John Wiley & Sons Inc., New York, 7th ed. 1978
4. Detailed information about the experiment see B. Abmayr: "Messung der Beweglichkeit von Ionenclustern unter Benutzung des 20 ms-Isomers  $^{24m}\text{Na}$  als Tracer", Diplomarbeit at the Technical University Munich, Department of Physics, January 1989.
5. see for example Vol XXII, part I, chapter 4 of K.Przibram: "Handbuch der Physik" (ed.: H. Geiger, K. Scheel), Verlag von Julius Springer, Berlin 1933
6. Blanc A.: Bull. Soc. Franc. de phys. 1908, p.156
7. Munson R.J., Tyndall A.M.: Proceedings of the Royal Society of London **A 172**, 28 (1939)
8. For detailed information on diffusion cloud chambers see e.g.: H. Slätis, Nucl. Instr. and Methods **1**, 213 (1957) or Katz J.L. et al., J. Chem. Phys. **62**, 448 (1975)
9. For study of nucleation in diffusion cloud chambers see e.g.: Rabeony H. et al., J. Phys. Chem. **91**, 1815 (1987)